Electron-impact single ionization of multiply charged aluminium ions



2001 J. Phys. B: At. Mol. Opt. Phys. 34 4113

(http://iopscience.iop.org/0953-4075/34/21/304)

INSTITUTE OF PHYSICS PUBLISHING JOURNAL OF PHYSICS B: ATOMIC, MOLECULAR AND OPTICAL PHYSICS

J. Phys. B: At. Mol. Opt. Phys. **34** (2001) 4113–4123 PII: S0953-4075(01)26279-8

# Electron-impact single ionization of multiply charged aluminium ions

**K Aichele[1], M Steidl[1], U Hartenfeller[1], D Hathiramani[1], F Scheuermann[1], M Westermann[1], E Salzborn[1] and M S Pindzola[2]**

[1] Institut für Kernphysik, Justus-Liebig-Universität, 35392 Giessen, Germany
[2] Department of Physics, Auburn University, Auburn, AL 36849, USA

E-mail: Salzborn@strz.uni-giessen.de

Received 21 June 2001, in final form 5 September 2001
Published 29 October 2001
Online at stacks.iop.org/JPhysB/34/4113

**Abstract**

Absolute total cross sections for electron-impact single ionization of $Al^{q+}$ ($q$ = 3–7) ions are investigated experimentally as well as theoretically. Employing the crossed-beams technique, the cross sections have been measured from below the respective ground state threshold up to 1 keV and partly up to 5.5 keV. The theoretical calculations were performed using the configuration-averaged distorted-wave method, including both direct ionization and excitation–autoionization contributions from the 2p-shell. The measurements are in good agreement with the calculations considering a small content of metastable ions in the incident ion beam. Because of the strong dominance by direct ionization processes the semiempirical Lotz formula can describe the measured data as well.

## 1. Introduction

The study of electron–ion collision phenomena is one of the main interests in modern atomic physics. Electron-impact ionization of ions is especially interesting for the fundamental understanding of plasma behaviour in astrophysics and controlled nuclear fusion (Griffin *et al* 1987, Müller 1991a). The need for atomic data to support fusion research has resulted in a wealth of cross sections for electron-impact ionization of ions (Phaneuf 1993). The knowledge of electron-impact cross section data of species encountered in the plasma is required for modelling the structure and dynamics of all kinds of high-temperature plasmas, especially in equal-temperature plasmas in which electron–ion collisions tend to dominate over ion–ion collisions. In fusion research the cross section data of metallic impurities such as titanium, chromium, iron, nickel, copper, molybdenum and tungsten are important (Müller 1991b, Gregory *et al* 1991). For most of these ions theoretical cross sections have been calculated over the last 15 years (e.g. Pindzola *et al* 1987, Griffin and Pindzola 1988). Also, experimental

  

cross section data for these metallic impurities of several isonuclear sequences have been measured (Gregory *et al* 1986, 1987, Stenke *et al* 1995a, 1995c, 1999, Hathiramani *et al* 1996, Hartenfeller *et al* 1998, Shaw *et al* 2001). Aluminium alloys are also a component of a fusion device and therefore its impurities can lead to energy loss in the hot plasma region by radiative cooling.

The atomic collision data for electron-impact single-ionization cross sections of Al ions are sparse. The only experimental data of aluminium electron-impact ionization cross sections are measured for $Al^{+}$ (Hayton and Peart 1994) and $Al^{2+}$ (Montague and Harrison 1983, Belic *et al* 1987, Crandall *et al* 1982). Theoretical calculations exist for both $Al^{+}$ (Griffin *et al* 1982, McGuire 1997) and $Al^{2+}$ (Badnell *et al* 1998). The main effort of investigating Al ions is for $Al^{2+}$, which is a member of the Na isoelectronic sequence. Such ions are of great interest in studies of ionization because they show resonance structures in the cross sections. Ionization rate coefficients have also been published for all Al ions (Voronov 1997). In order to expand the available atomic database and to test the accuracy of empirical and *ab initio* configuration-averaged distorted-wave (CADW) calculations, extensive measurements of cross sections for the electron-impact single ionization of $Al^{q+}$ ions in charge states $q = 3$–$7$ have been carried out. The ground configuration for all ions investigated has an outer subshell which is given by $2s^2 2p^k$ ($k = 2$–$6$).

The remainder of this paper is structured as follows. In section 2 we outline the crossed-beams experimental method, in section 3 we review distorted-wave theory as applied to the electron-impact ionization of atomic ions. In section 4 we compare experiment and theory for $Al^{3+}$ through $Al^{7+}$, while in section 5 we give a brief summary.

## 2. Experimental technique

The measurements were performed at the Giessen electron–ion crossed-beams set-up which has been described in detail previously (Tinschert *et al* 1989, Hofmann *et al* 1990). The $Al^{q+}$ ions were produced by evaporating aluminium from an oven into the plasma of a 10 GHz electron cyclotron resonance (ECR) ion source (Liehr *et al* 1993). The set-up of the oven is shown schematically in figure 1. A ceramic crucible filled with small pieces of the material intended for evaporation is heated indirectly by a tantalum foil (0.1 mm) mounted between two cylindrical, water-cooled copper electrodes. With this method ion currents of several $\mu$A could be obtained at an acceleration voltage of 12 kV. Another possibility for ion production is the insertion technique. Here, a bundle of thin Al wires is mounted on top of a rod fed axially to the edge of the ECR plasma. However, the ion currents we obtained were very low, therefore we used the oven method for the measurements.

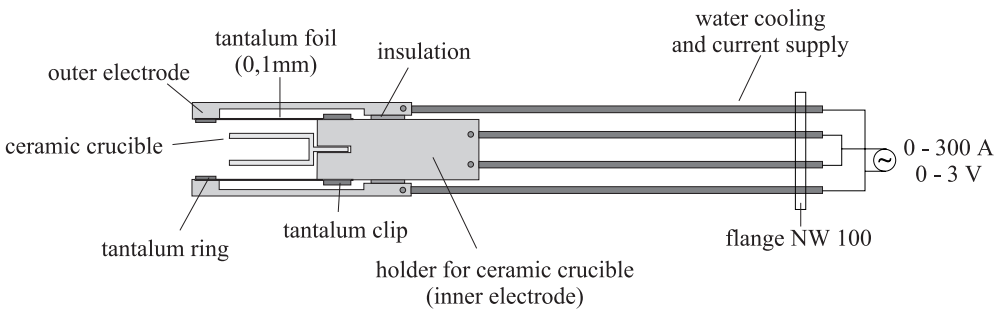


**Figure 1.** Schematic view of the evaporation oven.

After magnetic separation of the desired mass-to-charge ratio and tight collimation to typically 2 mm diameter, which reduced the beam current roughly by a factor of 100, the ion beam was crossed with an intense electron beam.

After the interaction the ionization products were separated magnetically from the incident ion beam and detected by a single-particle detector. The primary ion beam was collected in a large Faraday cup. To obtain absolute cross sections the dynamic crossed-beams technique was employed (Müller *et al* 1985) where the electron gun, i.e. the electron beam, is moved up and down across the ion beam with simultaneous registration of the ionization signal, the electron and the ion current. The typical measurement time is between 50 and 2000 s. The total experimental uncertainties of the measured cross sections are typically 8% at the maximum resulting from the quadrature sum of the non-statistical errors of about 7.8% and the statistical error at 95% confidence level.

We have used two different electron guns for the measurement. For electron energies up to 1 keV we applied a high-current electron gun designed by Becker *et al* (1985) for all investigated primary ions. This gun delivers a ribbon-shaped beam and an electron current of up to 450 mA at 1 keV. For the charge states $q = 5$–7 the additional use of a high-energy electron gun (Stenke *et al* 1995b) became necessary to extend the energy range beyond the cross section maxima up to energies of about 5.5 keV. This high-energy gun is designed in axial symmetry. The measured electron current increases in the normal mode from 1 mA at 100 eV up to 430 mA at 6.5 keV electron energy. Due to the experimental fact that the measured cross section depends on the gas pressure for normal measurements, another measurement mode for the electron gun was used for the experiment rather than that described by Stenke. We change the potentials of the gun electrode, so that the potential depression of the electronic space charge is not reduced or compensated by residual gas ions trapped in the electron beam. The cross section is no longer independent of the gas pressure in this mode (for details see Müller *et al* 1987). This reduces the current from 430 to 260 mA and the maximum electron energy to 5.5 keV due to the deflection of the electron beam. Furthermore, the electron energy has to be corrected after the measurement by typically 2.8% of the potential between the cathode and the potential of the interaction region. For details of the energy-scale calibration, which is accurate to better than 1 eV at 100 eV electron energy, we refer to Tinschert *et al* (1987).

## 3. Configuration-average distorted-wave method

The total ionization of the atomic ions in the Al isonuclear sequence should be dominated by contributions from direct 'knockout' ionization. Although time-dependent close-coupling and $R$-matrix pseudo-state calculations of direct ionization have been made for $Al^{2+}$ in the $1s^2 2s^2 2p^6 3s$ ground state configuration (Badnell *et al* 1998), their computational expense at this time precludes their application along a whole isonuclear sequence. Instead, we apply the configuration-averaged distorted-wave method (Pindzola *et al* 1986) to calculate direct ionization from the $1s^2 2s^2 2p^{6\rightarrow 2}$ ground state configurations of $Al^{3+}$ through $Al^{7+}$ and from the $1s^2 2s^2 2p^5 3s$ metastable excited configuration of $Al^{3+}$. The energies and bound orbitals for the Al configurations are calculated using the relativistic Hartree–Fock atomic structure code of Cowan (1981). The first-order perturbation theory expression for the direct ionization amplitude is reduced to a simple form by an algebraic average over all states of the initial configuration and an algebraic sum over all states of the final configuration. Thus the cross section is given by

$$\sigma_{\mathrm{tot}} = \sum_f \sigma_{\mathrm{ion}}(i \rightarrow f) + \sum_j \sigma_{\mathrm{exc}}(i \rightarrow j) \tag{1}$$

where $\sigma_{\rm ion}$ is the direct ionization cross section and $\sigma_{\rm exc}$ is the inner-shell excitation cross section.

We choose a form of the scattering amplitude which requires that the incident and scattered electrons are calculated in a $V^N$ potential, while the bound and ejected electrons are calculated in a $V^{N-1}$ potential (Younger 1980, Jakubowicz and Moores 1981). By direct comparison with non-perturbative theories (Badnell *et al* 1998), this particular first-order distorted-wave theory has been found to be fairly accurate for residual atomic ion charges greater than or equal to three. In addition, we expect that other first-order distorted-wave theories based on different choices of scattering potentials will be in good agreement with the direct ionization results presented below for $Al^{3+}$ through $Al^{7+}$. The smaller excitation–autoionization contributions to the total ionization cross sections for $Al^{3+}$ through $Al^{7+}$ are calculated by applying the configuration-averaged distorted-wave method to inner-shell excitation and assuming that the branching ratio for autoionization is approximately one.

The CADW method has been successfully applied to calculate excitation–autoionization contributions in many atomic ions with different complex electron configurations.

## 4. Comparison between experiment and theory

The cross sections for single ionization of $Al^{q+}$ ions in charge states $q = 3$–$7$ are shown in figures 2–6. The error bars represent the total experimental uncertainty. Beside the CADW calculations the experimental data are compared with the semiempirical Lotz formula (Lotz 1968), which is commonly used to estimate electron-impact single-ionization cross sections. The ionization potentials used in this formula are calculated using the multiconfigurational

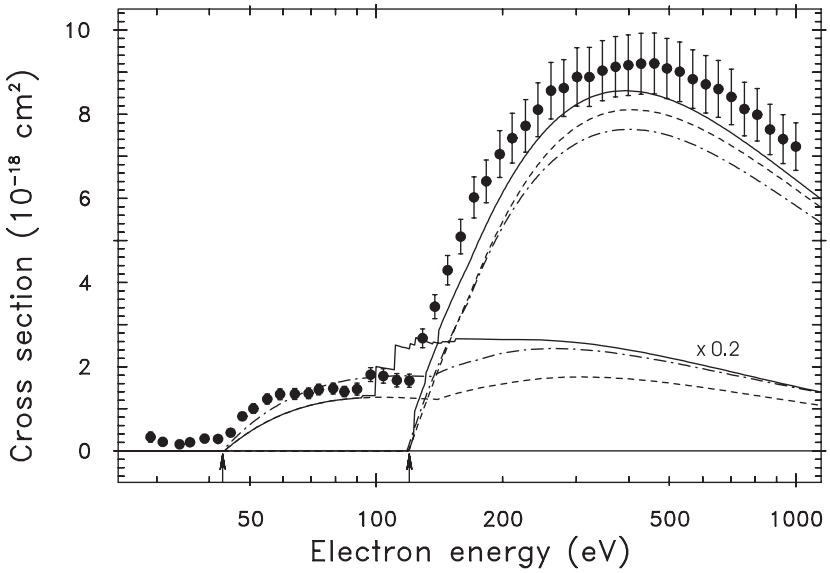


**Figure 2.** Total cross section for the single ionization of $Al^{3+}$ ions. Error bars represent the total experimental uncertainty. The arrows indicate the ionization thresholds of the excited metastable state $2p^5 3s$ at 43.1 eV (Grant *et al* 1980) and the ground state $2s^2 2p^6$ at 120.0 eV (Moore 1970). The curves for the excited state are scaled by a factor of 0.2. – – –, CADW calculation, direct ionization; ——, CADW calculation, total cross section (direct + EA); — · —, Lotz formula (Lotz 1968).

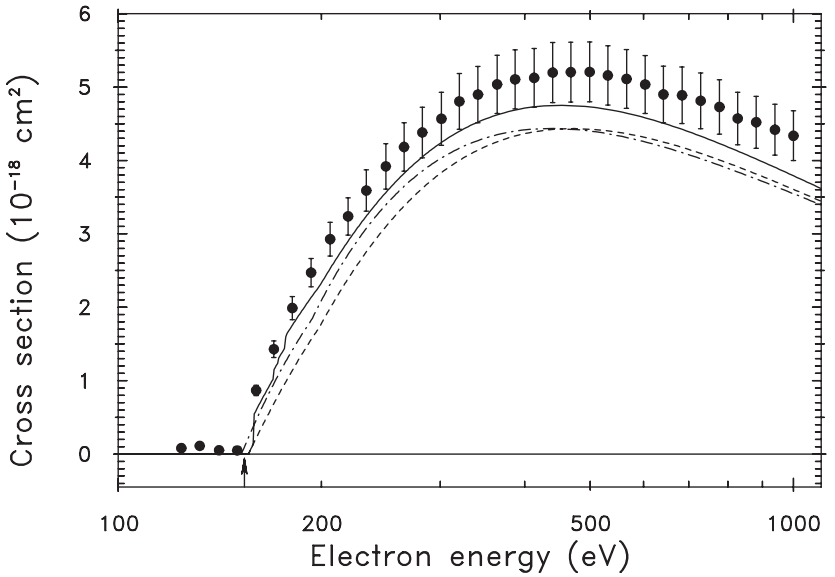


**Figure 3.** Total cross section for the single ionization of $Al^{4+}$ ions. Error bars represent the total experimental uncertainty. The arrow indicates the ionization threshold of the ground state $2s^22p^5$ at 153.7 eV (Moore 1970). – – –, CADW calculation, direct ionization; ——, CADW calculation, total cross section (direct + EA); — · —, Lotz formula (Lotz 1968).

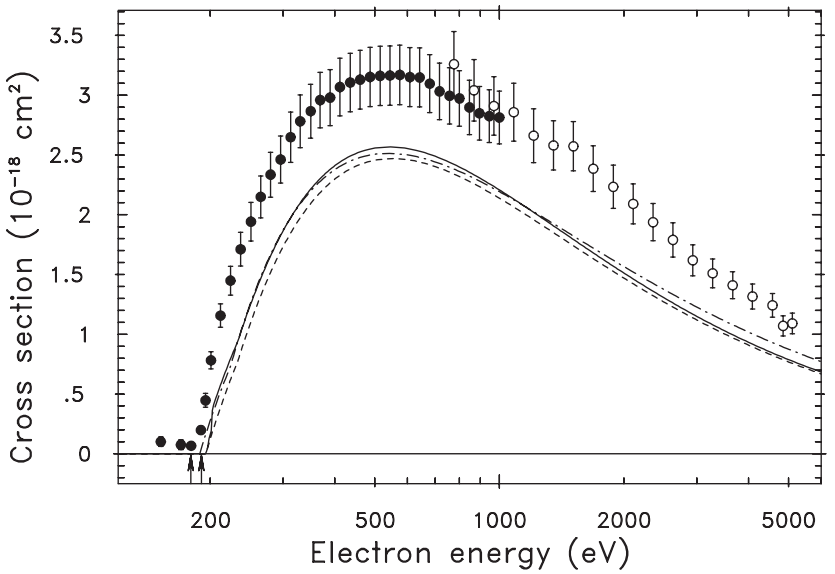


**Figure 4.** Total cross section for the single ionization of $Al^{5+}$ ions. Error bars represent the total experimental uncertainty. The arrows indicate the ionization thresholds of the states $(2s^22p^4)\ ^3P_2$ at 190.5 eV and $(2s^22p^4)\ ^1S_0$ at 179.5 eV, respectively (Moore 1970). ●, high-current electron gun; ○, high-energy electron gun; – – –, CADW calculation, direct ionization; ——, CADW calculation, total cross section (direct + EA); — · —, Lotz formula (Lotz 1968).

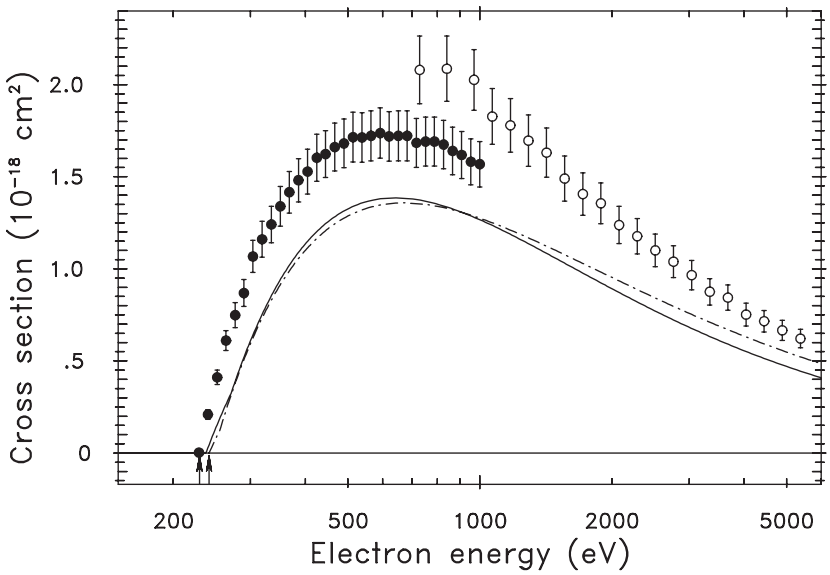


**Figure 5.** Total cross section for the single ionization of $Al^{6+}$ ions. Error bars represent the total experimental uncertainty. The arrows indicate the ionization thresholds of the states $(2s^2 2p^3)\ ^4S_{3/2}$ at 241.4 eV and $(2s^2 2p^3)\ ^2P_{3/2}$ at 229.7 eV, respectively (Moore 1970). ●, high-current electron gun; ○, high-energy electron gun; – – –, CADW calculation, direct ionization; ——, CADW calculation, total cross section; — · —, Lotz formula (Lotz 1968).

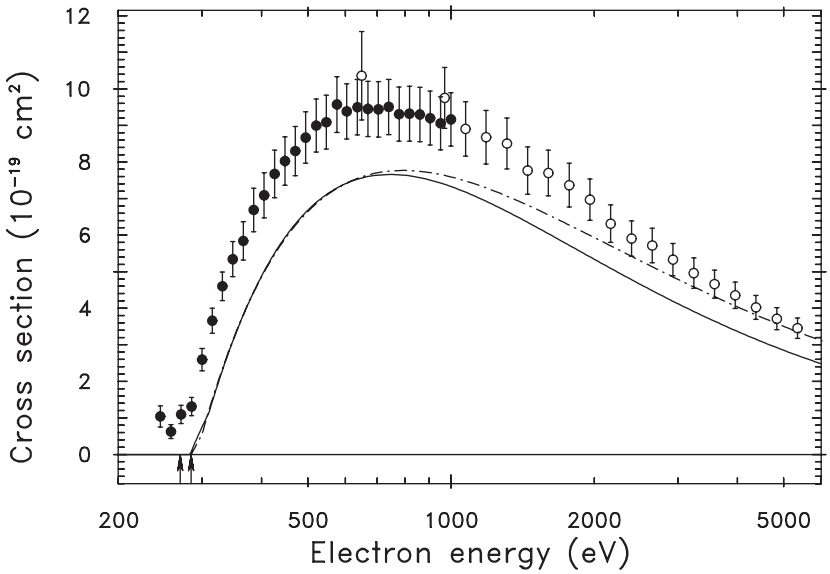


**Figure 6.** Total cross section for the single ionization of $Al^{7+}$ ions. Error bars represent the total experimental uncertainty. The arrows indicate the ionization thresholds of the states $(2s^2 2p^2)\ ^3P_0$ at 284.6 eV (Moore 1970) and $(2s^2 2p^2)\ ^1S_0$ at 269.9 eV (Grant *et al* 1980), respectively. ●, high-current electron gun; ○, high-energy electron gun; ——, CADW calculation, total cross section; — · —, Lotz formula (Lotz 1968).

**Table 1.** Threshold energies (eV) for the ionization of electrons in the subshells of aluminium ions.

| | | | Ionization potential | | |
|---|---|---|---|---|---|
| Ion | Configuration | Subshell | Grant | Cowan | Moore |
| $Al^{3+}$ | $1s^22s^22p^6$ | 2p | 118.4 | 119.6 | 120.0 |
| | | 2s | 165.3 | 166.4 | |
| $Al^{3+}$ | $1s^22s^22p^53s$ | 3s | | 43.57 | |
| | | 2p | | 139.2 | |
| | | 2s | | 200.8 | |
| $Al^{4+}$ | $1s^22s^22p^5$ | 2p | 152.2 | 155.9 | 153.7 |
| | | 2s | 193.4 | 198.8 | |
| $Al^{5+}$ | $1s^22s^22p^4$ | 2p | 188.8 | 195.3 | 190.5 |
| | | 2s | 223.5 | 233.7 | |
| $Al^{6+}$ | $1s^22s^22p^3$ | 2p | 241.5 | 237.6 | 241.4 |
| | | 2s | 255.6 | 270.8 | |
| $Al^{7+}$ | $1s^22s^22p^2$ | 2p | 284.7 | 283.0 | 284.6 |
| | | 2s | 299.6 | 310.1 | |

Dirac–Fock-code of Grant (Grant *et al* 1980). The results of these calculations are listed in table 1 together with results obtained using the relativistic Hartree–Fock atomic structure code of Cowan (1981) and available experimental data published by Moore (1970).

### *4.1. $Al^{3+}$*

In figure 2 the cross section for single ionization of $Al^{3+}$ is shown. Below the ionization threshold of the ground state $2s^22p^6$ at 119.6 eV a significant onset of the ionization signal can be seen above 42 eV. Obviously, this is caused by long-lived, excited ions which are also produced in the ECR ion source and therefore the $Al^{3+}$ ion beam used for the measurements has a fraction of metastable ions. CADW calculations confirm the threshold for metastable ions in the $2p^53s$ configuration at 43.4 eV. The transition of $Al^{3+}$ ions in the $2p^53s\ ^3P$ state to the $2s^22p^6\ ^1S$ ground state is dipole-forbidden and, therefore, these metastable ions contribute significantly to the cross section of $Al^{3+}$.

For the estimation of the component of metastable ions in the incident beam both the Lotz formula and the CADW calculations for the $2p^53s$ state are scaled by a factor of 0.2 to fit them to the data points below the ground state threshold. Therefore, one can conclude that the incident beam contains a metastable ion fraction of 20%.

The CADW calculation for the ground state ionization considers direct 2s- and 2p-ionization and additionally a small content of $2s \rightarrow 3\ell$ excitation–autoionization processes. For the cross section of the metastable $2p^53s$ configuration both direct ionization from the 3s-, 2p- and 2s-shells and $2p \rightarrow 3\ell$ and $2p \rightarrow 4\ell$ excitation–autoionization processes are taken into account. The calculated excitation energies can be seen in table 2. The measured cross section corresponds fairly well with the above-mentioned calculation for the ground state, whereas it is expected for a primary ion beam which is clean of metastable ions that the calculations would slightly overestimate the measurement. The data around 100 eV pointed to the calculated $2p \rightarrow 3p$ excitation–autoionization process but the similarly strong contribution to the calculated cross section from $2p \rightarrow 3d$ excitation cannot be seen in the measurement. However, the role of excitation–autoionization is not so important in this case as for heavy ions, as can be seen in figure 2. The Lotz formula (Lotz 1968) is often used for cross

**Table 2.** Results of the excitation energies of the CADW calculations for the ground state of $Al^{3+}$ ($2s^22p^6$) and the $2s^22p^53s$ metastable state.

| Electron configuration | Process | Energy (eV) |
|---|---|---|
| $Al^{3+}$ ($2s2p^63s$) | 2s → 3s excitation | 123.23 |
| $Al^{3+}$ ($2s2p^63p$) | 2s → 3p excitation | 130.96 |
| $Al^{3+}$ ($2s2p^63d$) | 2s → 3d excitation | 140.82 |
| $Al^{3+}$ ($2s^22p^43s^2$) | 2p → 3s excitation | 92.40 |
| $Al^{3+}$ ($2s^22p^43s3p$) | 2p → 3p excitation | 99.50 |
| $Al^{3+}$ ($2s^22p^43s3d$) | 2p → 3d excitation | 111.00 |
| $Al^{3+}$ ($2s^22p^43s4s$) | 2p → 4s excitation | 117.27 |
| $Al^{3+}$ ($2s^22p^43s4p$) | 2p → 4p excitation | 120.33 |
| $Al^{3+}$ ($2s^22p^43s4d$) | 2p → 4d excitation | 124.04 |
| $Al^{3+}$ ($2s^22p^43s4f$) | 2p → 4f excitation | 125.08 |
| $Al^{3+}$ ($2s2p^53s^2$) | 2s → 3s excitation | 136.14 |
| $Al^{3+}$ ($2s2p^53s3p$) | 2s → 3p excitation | 142.87 |
| $Al^{3+}$ ($2s2p^53s3d$) | 2s → 3d excitation | 154.32 |

**Table 3.** Results of the CADW calculations of the excitation energies for the $2s^22p^5$ ground state of $Al^{4+}$.

| Electron configuration | Process | Energy (eV) |
|---|---|---|
| $Al^{4+}$ ($2s2p^53d$) | 2s → 3d excitation | 158.74 |
| $Al^{4+}$ ($2s2p^54s$) | 2s → 4s excitation | 169.47 |
| $Al^{4+}$ ($2s2p^54p$) | 2s → 4p excitation | 172.63 |
| $Al^{4+}$ ($2s2p^54d$) | 2s → 4d excitation | 176.57 |
| $Al^{4+}$ ($2s2p^54f$) | 2s → 4f excitation | 177.43 |

section estimations and is a good approximation for the direct ionization process. Therefore, it describes the measured data as well as the CADW calculations within its error.

### *4.2. $Al^{4+}$ and $Al^{5+}$*

The measurements for the electron-impact ionization cross section of $Al^{4+}$ (ground state configuration $2s^22p^5$) are compared with the distorted-wave theory and the Lotz formula in figure 3. Calculations are made for direct ionization from the $2s^22p^5$ ground state configuration including both the 2p and 2s subshells. Furthermore, 2s → 3d and 2s → 4$\ell$ ($\ell$ = 1–2) excitation energies and their excitation–autoionization cross sections were calculated. The excitation energies are given in table 3. The onset corresponds very well with the predicted ionization threshold at 153.7 eV given by Moore (1970) and our calculated threshold at 155.9 eV (Cowan 1981) and 152.2 eV (Grant *et al* 1980). Therefore, it can be concluded that nearly all ions in the incident beam were in the ground state configuration. The indirect contributions to the cross section of $Al^{4+}$ are the largest (compared with the other investigated $Al^{q+}$-cross sections (for the ground state)). Nevertheless, the total contribution of excitation–autoionization processes to the total cross section is lower than 8%. Again the deviations between the experimental data, the CADW calculation and the Lotz formula are small.

This can also be seen in the cross section for $Al^{5+}$ in figure 4. Furthermore, excitation–autoionization processes (see table 4) do not contribute significantly to the cross section. In the cross section maximum the measurement is underestimated by the theory by 20%. In the figure one can also see that the onset of the ionization signal is slightly below the ($2s^22p^4$) $^3P_2$ ground

**Table 4.** Results of the CADW calculations of the excitation energies for the $2s^22p^4$ ground state of $Al^{5+}$.

| Electron configuration | Process | Energy (eV) |
|---|---|---|
| $Al^{5+}$ ($2s2p^44p$) | $2s \rightarrow 4p$ excitation | 197.58 |
| $Al^{5+}$ ($2s2p^44d$) | $2s \rightarrow 4d$ excitation | 201.66 |
| $Al^{5+}$ ($2s2p^44f$) | $2s \rightarrow 4f$ excitation | 202.81 |

state threshold (190.5 eV). The ions in the ion beam, which were in the same configuration but in the $^1S_0$ state, could be the reason for the enhancement of the cross section and for the small but visible earlier onset of the cross section at 179.5 eV. For this cross section the energy range was extended to 5000 eV by the high-energy electron gun. The agreement of the two independent experiments in the overlap region is within the error bars, so that we conclude that a similar population of the states was established during the measurement. At 1500 eV, a small rise of the cross section can be observed. Energy calculations (Grant *et al* 1980) are able to explain this small step as a $1s \rightarrow n\ell$ excitation–autoionization process, where the lowest excitation threshold ($1s \rightarrow 2p$) lies at 1500.7 eV. Cross section calculations for this process were not performed.

### *4.3. $Al^{6+}$ and $Al^{7+}$*

The theoretical ionization threshold for single ionization of the ground state of $Al^{6+}$ is 237.6 (Cowan 1981) and 241.5 eV (Grant *et al* 1980) (table 1). Moore's (1970) tables give 241.4 eV. As for $Al^{5+}$, the energy levels of the states in the ground state configuration differ by a few eV. However, the rise of the cross section of $Al^{6+}$ begins at about 230 eV (figure 5). Obviously there is a small content of metastable ions in the ($2s^22p^3$) $^2P_{3/2}$ state, whose ionization threshold is at 229.7 eV. This metastable content in the ion beam leads to an enhanced cross section, as was also observed for $Al^{5+}$. Note that the theoretical (CADW) cross section for $Al^{6+}$ only includes the direct ionization. This does not mean that excitation–autoionization processes are negligible, but the relative contribution to the cross section is low. However, the deviation of the theory compared with the experimental data is similar to that observed for $Al^{5+}$ ions, as well as compared with the Lotz (1968) formula. Noticeable in figure 5 is the disagreement of the experimental results in the energy overlap range used by both guns. An explanation for this could be a small shift of the cathode position due to thermal expansion relative to the pierced electrode. We know from tests that this mainly affects the emission and the trajectory of the electrons and this has an influence on the cross section measurement. However, this effect was not observed for the other cross section measurements ($Al^{5+}$ and $Al^{7+}$) performed using the high-energy gun.

For the highest charge state measured in this work, $Al^{7+}$, the agreement in the energy overlap range of both guns used is good (figure 6). The CADW calculations were carried out only for the direct ionization and describe the general shape of the cross section function very well, although they are about 20% too small in absolute value. Below the $^3P_0$ ($2s^22p^2$) ground state ionization threshold at 284.6 eV again a remarkable ionization signal can be observed. Metastable ions in the $^1S_0$ state of the same configuration can contribute above 269.9 eV, but in this case it is not clear whether there is an experimental ionization threshold, because even below this energy there is a small ionization signal. Other metastable ions in the ion beam could cause this ionization signal.

## 5. Summary

In this paper, we have reported for the first time on crossed-beams measurements and configuration-averaged distorted-wave calculations of electron-impact single-ionization cross sections for $Al^{q+}$ ions in charge states $q = 3$–7. A non-vanishing fraction of ions in long-lived, metastable states produced in the plasma of the ECR ion source was observed in the primary ion beams. For $q = 3$, the measurement shows a relative large contribution from such metastable ions in an electron configuration other than the respectively ground state. For the other ions measured, the fractions of metastable ions seem to be small. In these cases, the metastable states of the ions investigated have the same electron configuration as the ground state.

Comparison between CADW calculations and the experimental data shows that the contributions from direct ionization dominate the cross sections with increasing charge state. Excitation–autoionization processes do not play an important role. Therefore, the semiempirical Lotz formula describes the measurement quite well.

## Acknowledgments

Support by the Deutsche Forschungsgemeinschaft (DFG), Bonn–Bad Godesberg, is gratefully acknowledged. The authors thank A Diehl for helpful discussions.

## References

Badnell N R, Pindzola M S, Bray I and Griffin D C 1998 *J. Phys. B: At. Mol. Opt. Phys.* **31** 911
Becker R, Müller A, Achenbach C, Tinschert K and Salzborn E 1985 *Nucl. Instrum. Methods* B **9** 385
Belic D S, Falk R A, Timmer C and Dunn G H 1987 *Phys. Rev.* A **36** 1073
Cowan R D 1981 *The Theory of Atomic Structure and Spectra* (Berkeley, CA: University of California)
Crandall D H, Phaneuf R A, Falk R A, Belic D S and Dunn G H 1982 *Phys. Rev.* A **25** 143
Grant I P, McKenzie B J, Norrington P H, Mayers D F and Pyper N C 1980 *Comput. Phys. Commun.* **21** 207
Gregory D C, Hahn Y, Müller A, Abramov V A, Badnell N R, Berrington K, Bitter M and Shevelko V P 1991 *Phys. Scr.* T **37** 8
Gregory D C, Meyer F W, Müller A and Defrance P 1986 *Phys. Rev.* A **34** 3657
Gregory D C, Wang L J, Meyer F W and Rinn K 1987 *Phys. Rev.* A **35** 3256
Griffin D C and Pindzola M S 1988 *J. Phys. B: At. Mol. Opt. Phys.* **21** 3253
Griffin D C, Pindzola M S and Bottcher C 1982 *Phys. Rev.* A **25** 154
——1987 *Phys. Rev.* A **36** 3642
Hartenfeller U, Aichele K, Hathiramani D, Hofmann G, Schäfer V, Steidl M, Stenke M, Salzborn E and Pindzola M S 1998 *J. Phys. B: At. Mol. Opt. Phys.* **31** 2999
Hathiramani D *et al* 1996 *Phys. Rev.* A **54** 587
Hayton S J T and Peart B 1994 *J. Phys. B: At. Mol. Opt. Phys.* **27** 5331
Hofmann G, Müller A, Tinschert K and Salzborn E 1990 *Z. Phys.* D **16** 113
Jakubowicz H and Moores D L 1981 *J. Phys. B: At. Mol. Phys.* **14** 3733
Liehr M, Schlapp M, Trassl R, Hofmann G, Stenke M, Völpel R and Salzborn E 1993 *Nucl. Instrum. Methods* B **79** 697
Lotz W 1968 *Z. Phys.* **216** 241
McGuire E J 1997 *J. Phys. B: At. Mol. Opt. Phys.* **30** 1563
Montague R G and Harrison M F A 1983 *J. Phys. B: At. Mol. Phys.* **16** 3045
Moore C E 1970 *Ionization Potentials and Ionization Limits derived from the Analysis of Optical Spectra (NSRDS-NBS 34)* (Washington, DC: US Govt Printing Office)
Müller A 1991a *Physics of Ion Impact Phenomena* ed D Mathur (Berlin: Springer) p 13
——1991b *Phys. Scr.* T **37** 14
Müller A, Hofmann G, Tinschert K, Sauer R and Salzborn E 1987 *Nucl. Instrum. Methods* B **24/25** 269
Müller A, Tinschert K, Achenbach C, Salzborn E and Becker R 1985 *Nucl. Instrum. Methods* B **10/11** 204
Phaneuf R A 1993 *Phys. Scr.* T **47** 124

Pindzola M S, Griffin D C and Bottcher C 1986 *Atomic Processes in Electron–Ion and Ion–Ion Collisions (NATO ASI Series B 145)* p 75
——1987 *Comment. At. Mol. Phys.* **20** 337
Shaw J A, Pindzola M S, Steidl M, Aichele K, Hartenfeller U, Hathiramani D, Scheuermann F, Westermann M and Salzborn E 2001 *Phys. Rev.* A **63** 032709
Stenke M, Aichele K, Hartenfeller U, Hathiramani D, Steidl M and Salzborn E 1995a *J. Phys. B: At. Mol. Opt. Phys.* **28** 2711
——1999 *J. Phys. B: At. Mol. Opt. Phys.* **32** 3627
Stenke M, Aichele K, Hathiramani D, Hofmann G, Steidl M, Völpel R and Salzborn E 1995b *Nucl. Instrum. Methods* B **98** 573
Stenke M, Hathiramani D, Hofmann G, Shevelko V P, Steidl M, Völpel R and Salzborn E 1995c *Nucl. Instrum. Methods* B **98** 138
Tinschert K, Müller A, Hofmann G, Achenbach C, Becker R and Salzborn E 1987 *J. Phys. B: At. Mol. Phys.* **20** 1121
Tinschert K, Müller A, Hofmann G, Huber K, Becker R, Gregory D C and Salzborn E 1989 *J. Phys. B: At. Mol. Opt. Phys.* **22** 531–40
Voronov G S 1997 *At. Nucl. Data Tables* **65** 1
Younger S M 1980 *Phys. Rev.* A **22** 111